

Invited paper

Leonardo Scarabelli*

Recent advances in the rational synthesis and self-assembly of anisotropic plasmonic nanoparticles

<https://doi.org/10.1515/pac-2018-0510>

Abstract: The field of plasmonics has grown at an incredible pace in the last couple of decades, and the synthesis and self-assembly of anisotropic plasmonic materials remains highly dynamic. The engineering of nanoparticle optical and electronic properties has resulted in important consequences for several scientific fields, including energy, medicine, biosensing, and electronics. However, the full potential of plasmonics has not yet been realized due to crucial challenges that remain in the field. In particular, the development of nanoparticles with new plasmonic properties and surface chemistries could enable the rational design of more complex architectures capable of performing advanced functions, like cascade reactions, energy conversion, or signal transduction. The scope of this short review is to highlight the most recent developments in the synthesis and self-assembly of anisotropic metal nanoparticles, which are capable of bringing forward the next generation of plasmonic materials.

Keywords: anisotropy; gold nanoparticles; IUPAC-SOLVAY International Award for Young Chemists; optical tweezers; plasmonics; seeded-growth; self-assembly; surface-enhanced Raman scattering.

Introduction

Nanotechnology represents the next scientific revolution and the biggest technological leap in human history, providing groundbreaking solutions in almost every aspect of modern lives, leading to faster computers, improved security, longer lifetimes, and a cleaner Earth. According to the Engineering and Physical Sciences Research Council, two of the grand challenges in materials science for the next century are “assembling and control at the nanoscale” as well as the “smart design of functional materials” [1]. At its core, nanotechnology asserts that “less is different”, meaning that when decreasing materials size down to the nanoscale, a whole family of new phenomena arises, with the need for a new level of description [2]. In the case of metallic nanoparticles, the emergence of plasmons is the most striking phenomena, and plasmonics has become one of the most active branches of nanotechnology, and the field has rapidly merged into different disciplines, gathering the interest of scientists and engineers of diverse backgrounds [3–10].

Plasmons: the interaction of metallic nanoparticles with light

Michael Faraday authored the first published scientific study on the optical properties of thin films and colloidal suspensions of gold particles in 1857. This work was an attempt by Faraday to explain the nature of

Article note: A collection of peer-reviewed articles by the winners of the 2017 IUPAC-SOLVAY International Award for Young Chemists.

*Corresponding author: **Leonardo Scarabelli**, Department of Chemistry and Biochemistry, University of California, California NanoSystems Institute, Los Angeles, CA, USA, e-mail: lscarabelli@ucla.edu

the Purple of Cassius, a metal nanoparticle-based pigment that dates back to the seventeenth century [11]. Faraday concluded that the different colorations were directly linked to the dimensions of the gold particles and the thickness of the thin films, he described for the first time the intrinsic thermodynamic instability of gold colloids, and discovered the first synthetic and stabilization process of gold nanoparticles in water [12, 13]. Within the following century, the fundamental physical comprehension of plasmon generation was achieved. Today, a plasmon is more generally defined as the collective oscillation of conduction band electrons induced by an external electromagnetic field. This interaction is described by the dielectric function of a material, and for metals, this can be approximated using the Drude-Lorentz model, in which the electrons are treated like a cloud of charged particles and the metal nuclei are considered fixed [14–16]. If the metal object is smaller than the excitation wavelength, its electron cloud reacts coherently to the external field, and the phenomenon takes the name of localized surface plasmon resonance (LSPR, Fig. 1a) [15–17]. Another important consequence of the reduced size of the probed particle is that the spatial dependence of the external electromagnetic field can be ignored, and the system can be described under the *quasi-static* approximation regime [14, 18, 19]. Using these approximations, Gustav Mie derived the extinction cross section of a plasmon in 1908, solving Maxwell's equations for the case of a nanoscale metal sphere immersed in an electromagnetic field [16, 17, 20]:

$$\sigma_{\text{ext}}(\omega) = \frac{24\pi^2 R^3 \cdot \epsilon_m^{3/2}}{\lambda} \frac{\epsilon_2(\omega)}{[\epsilon_1(\omega) + 2\epsilon_m]^2 + \epsilon_2(\omega)^2} \quad (1)$$

where $\sigma_{\text{ext}}(\omega)$ is the extinction cross-section, $\epsilon_1(\omega)$ and $\epsilon_2(\omega)$ are the real and imaginary parts of the dielectric function of the metal, ϵ_m is the dielectric constant of the embedding medium, R is the radius of the particle, and λ is the wavelength of the electromagnetic radiation. Here, the maxima of eq. (1) identify the resonance conditions for generating LSPR, associated with the spectral absorption band at a specific peak wavelength.

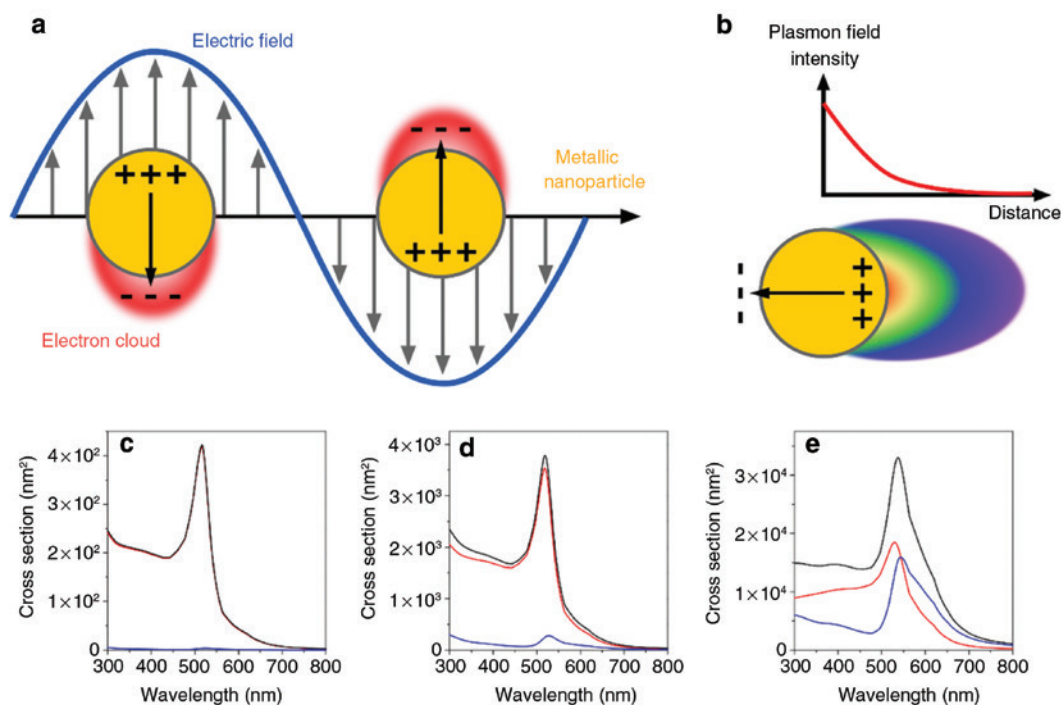


Fig. 1: Interaction of metal nanoparticles with light. (a) Schematic representation of the effect of an incoming electromagnetic wave on the electron cloud of a spherical nanoparticle. (b) Schematic representation of a plasmonic field decaying with distance from the metal surface. (c–e) Extinction (black line), absorption (red line) and scattering (blue line) cross-section for gold nanoparticle of different diameter: (c) 20 nm, (c) 40 nm and (d) 80 nm.

An important consequence of plasmon excitation is the confinement of a localized electric field at the surface of the metal, which is significantly more intense than the one associated with the external excitation (Fig. 1b) [16]. This plasmon-generated electromagnetic field represents the heart of surface-enhanced phenomena, such as surface-enhanced Raman scattering (SERS) [21–23], surface-enhanced infrared absorption (SEIRA) [24], and surface-enhanced fluorescence (SEF) [25]. Similar expressions to eq. (1) can be written for scattering cross-section. Consequently, both scattering and extinction cross-sections depend on particle size where their ratios vary as $1/R^3$. As such, the contribution of scattering increases for bigger particles, as illustrated in Fig. 1c–e using boundary element method (BEM) simulations [26]. As a direct consequence of this relationship, the interacting photon can either be scattered or absorbed by the metal nanoparticle. Scattering effects are used for single-particle spectroscopy, sensing, and generation of optical nano-antennas and waveguides with low heat generation. On the other hand, absorption is used for photothermal applications, energy conversion and photocatalysis [27]. All of these applications rely on the capability of precisely engineering plasmon resonance conditions to generate plasmonic bands with a desired wavelength, and harvest photons in a broad range of frequencies from the middle infrared to the ultraviolet [28, 29].

Synthesis of anisotropic plasmonic nanoparticles

With the start of the new millennium, the introduction of the seeded growth synthesis approach brought about a major turning point by providing access to an exceptional variety of shapes, including rods, wires, stars, cubes, tetrahedra, and more irregular branched structures. This method involves two physically and temporally separated steps: the synthesis of small metal nanoparticle seeds (<5 nm), and their dispersion in a growth solution [30–35]. The capability for independent nucleation and growth optimization of the metal crystals has resulted in an unprecedented level of control over nanoparticle size and shape [30, 33, 34, 36–38]. These advances have established seeded-growth protocols as the most commonly used for anisotropic metal nanoparticle synthesis, and it has been the subject of many reviews [36, 39–44]. With the seeded-growth method, the morphology of the final product can be controlled with size and shape of the seed, concentration of the capping agents in the growth solution, and ratio of the metal salt to reductant [31, 32, 39, 42, 45]. Some of the most common shapes are summarized in Fig. 2, together with their plasmonic properties. The effect of nanoparticle shape on plasmonic properties can be mathematically determined by applying Mie's theory to an ellipsoid having three axes $a=b \neq c$, leading to two different resonance conditions [15, 16]. This is experimentally verified with nanorods, which display transverse and longitudinal plasmon bands (Fig. 2d,f) [46]. Additionally, shape anisotropy dictates which crystal facets dominate the surface of the final product. These domains have drastic consequences on electronic conductivity, catalytic activity, and surface reactions [30–32, 39, 47–51].

The importance of seed size and crystallinity for the controlled growth of well-defined and homogeneous nanoparticles became evident a few years following the introduction of the first seed-growth method [31, 52, 53]. However, unlike the efforts that were canalized in the optimization of growth conditions, the protocol for seed preparation has remained comparatively unchanged. These considerations suggest that more robust methods for seeds synthesis, and an improved understanding of their evolution during particle growth will facilitate the design of novel synthetic protocols. Many groups explored this direction in the last 5 years: Niu *et al.* and O'Brien *et al.* both demonstrated an iterative growth/etching cycle that can be used to prepare homogeneous single-crystal gold seeds, reducing both the amount of by-products and the size dispersity of grown particles [54, 55]. This strategy was extended by Liz-Marzán's group where gold nanorods and triangular nanoprisms were utilized as starting materials to produce well-defined single-crystalline and mono-twinned seeds, respectively [56–58]. This enabled the systematic investigation of seed size and twinning grade on the shape evolution of gold nanoparticles changing the growth media (Fig. 3). The most significant finding of this study is that twin-defects can be introduced during growth, but cannot be removed. Furthermore, this work indicated that the growth process is size-dependent, which suggests that the optimization of these protocols should be focused on employing larger seeds with a more stable crystallographic structure in the desired growth conditions [56].

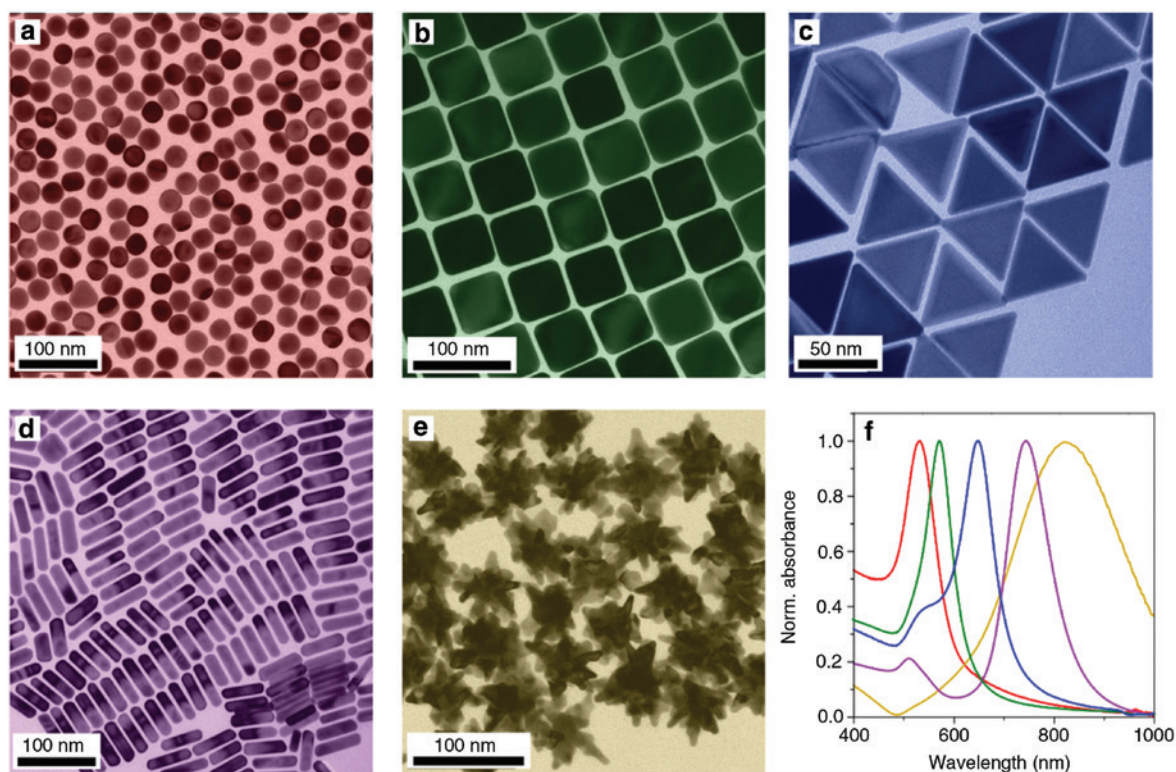


Fig. 2: Examples of gold metal nanoparticle shapes seen through transmission electron microscopy. (a) Nanospheres, (b) nanohexahedrons (i.e. cubes), (c) nanotriangles, (d) nanorods, (e) nanostars, (f) UV-visible spectra showing the optical properties of the different nanoparticle shapes presented in panels (a–e): nanospheres (red), nanohexaedrons (green), nanotriangles (blue), nanorods (purple), nanostars (yellow). The plasmonic properties of each shape can be further tuned changing nanoparticle size and aspect ratio.

In the same year, Liz-Marzán's group also optimized a mild thermal treatment on small citrate-capped gold nanoparticles to increment the population of penta-twinned seeds [59]. Remarkably, this protocol improved the shape-yield for gold bipyramids, penta-twinned nanorods, and decahedra above 90 % (Fig. 4a–c) [60]. Moreover, the prepared seeds displayed improved long-term stability and remained functional for several months, instead of being prepared freshly for every synthesis, one of the common problems with seeded-growth methods. They also took advantage of state-of-the-art electron tomography analyses [61–63], superimposing low and high angle annular dark field scanning transmission electron microscopy (LAADF- and HAADF-STEM) in a dose-efficient manner. This approach enabled the characterization of the gold nanoparticle internal structure, identifying crystal planes and twin defects (Fig. 4d) [64]. Additionally, this technique combined with energy dispersive X-ray spectroscopy (EDS or EDX) allowed the identification of the position of the original seed (coated with a thin layer of palladium) inside the grown particle (Fig. 4e–g) [60, 64]. The growth of the gold crystal around the seed resulted to be heavily dependent on the percentage of palladium introduced and on the shape of the final product, giving new insight into the mechanistic aspect of symmetry breaking and anisotropic nanoparticle growth (Fig. 4h).

Exploring new types of ligands and surfactants employed in the synthesis of gold nanostructures is another aspect that requires new insights. Although physicochemical properties such as carbon chain length, charge, and concentration have been analyzed in great detail [65–70], and the combination of additives has been explored [58, 71, 72], the collection of compounds that are typically used as stabilizers for colloidal suspensions of nanoparticles is still incredibly limited. In a recent publication in *Nature*, Lee *et al.* reported the introduction of chiral ligands in the growth mixture for the synthesis of enantiomerically pure gold nanoparticles, and demonstrated unprecedented control over their chiral plasmonic properties (Fig. 5a–c) [73].

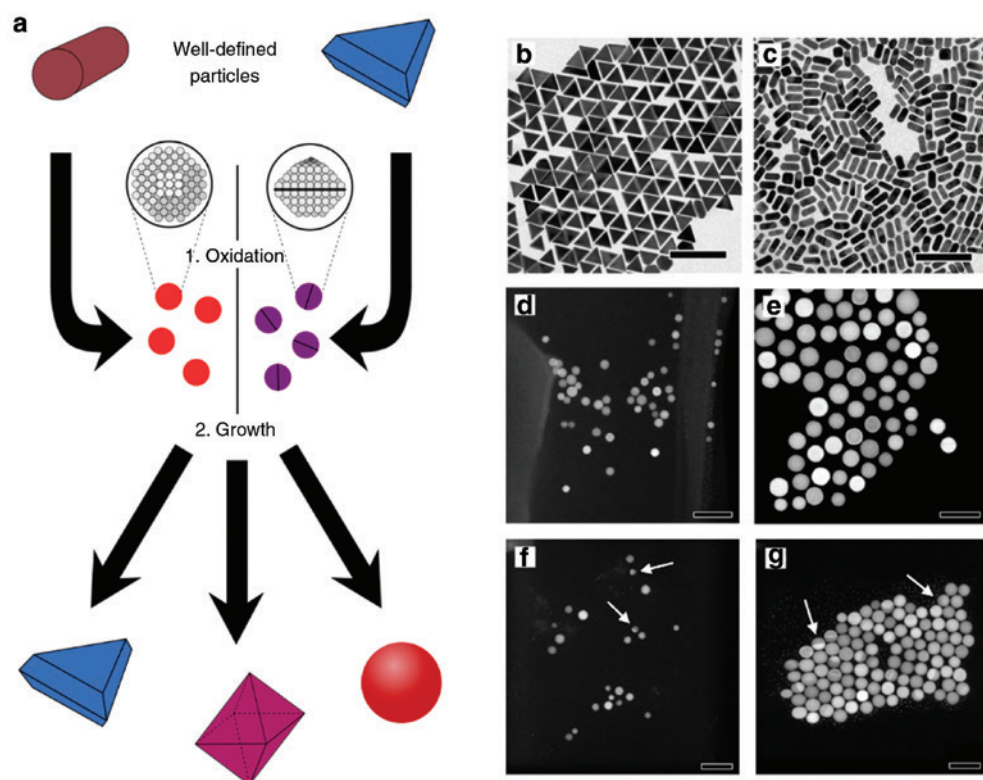


Fig. 3: Role of the seeds for the growth of gold nanoparticles of different morphologies. (a) Schematic representation of the experimental procedure used to systematically study the role of size and twinning in the growth of gold nanoparticles. (b,c) TEM images of the starting nanotriangles (b) and nanorods (c). (d–g) Angular dark field scanning TEM images of seeds obtained from the oxidative etching of nanorods [12 nm, (d), and 20 nm, (e)], and nanotriangles [12 nm, (f), and 20 nm, (g)]. Diffraction contrast is present, which indicates the presence of twins (as indicated in some representative particles by white arrows). In the case of the single crystal seeds obtained from gold nanorods, twins could not be observed for the vast majority of the analyzed particles. Scale bars: (b,c) 200 nm; (d–g) 50 nm. Adapted with permission from Ref. [56] – Published by The Royal Society of Chemistry.

While enantiomers and enantioselectivity are ubiquitous concepts in biological systems and biochemical reactions, the study of plasmon chirality has been hindered by synthetic limitations involving enantiomerically pure plasmonic products. Although various groups have reported strong chiral effects in different plasmonic assemblies, facile methods for the large-scale production of three-dimensional chiral structures has remained elusive [74–78]. Lee *et al.* utilized a straightforward approach in introducing selective handedness through the addition of cysteine and cysteine-containing peptides in the growth media [73]. These molecules bind to intrinsically chiral ‘kink’ sites present on high-index facets of growing crystals (Fig. 5d,e) [79, 80]. Remarkably, the obtained chiral optical activity (g-factor 0.2) is orders of magnitude higher than those associated with previously reported particle assemblies, small molecules, or proteins. Further development of these synthetic strategies will have important implications in the fabrication of three-dimensional chiral nanostructures for the rational design of artificial chirality and chiro-optical properties for active color displays, holography, reconfigurable switching, chirality sensing, and all-angle negative-refractive-index plasmonic materials.

Another general approach for tailoring the plasmonic properties of anisotropic gold colloids is the post-synthetic modification of the nanoparticle shape with overgrowth [58, 81–83], oxidative etching [84, 85], and epitaxial deposition [29, 86, 87]. In a ground-breaking work published last year in *Science*, González-Rubio *et al.* explored an unconventional approach by demonstrating the possibility of refining gold nanorod suspensions using a femtosecond pulsed laser. This innovative methodology demonstrates the potential for tuning the final optical properties of the collective colloid assembly close to those computationally predicted

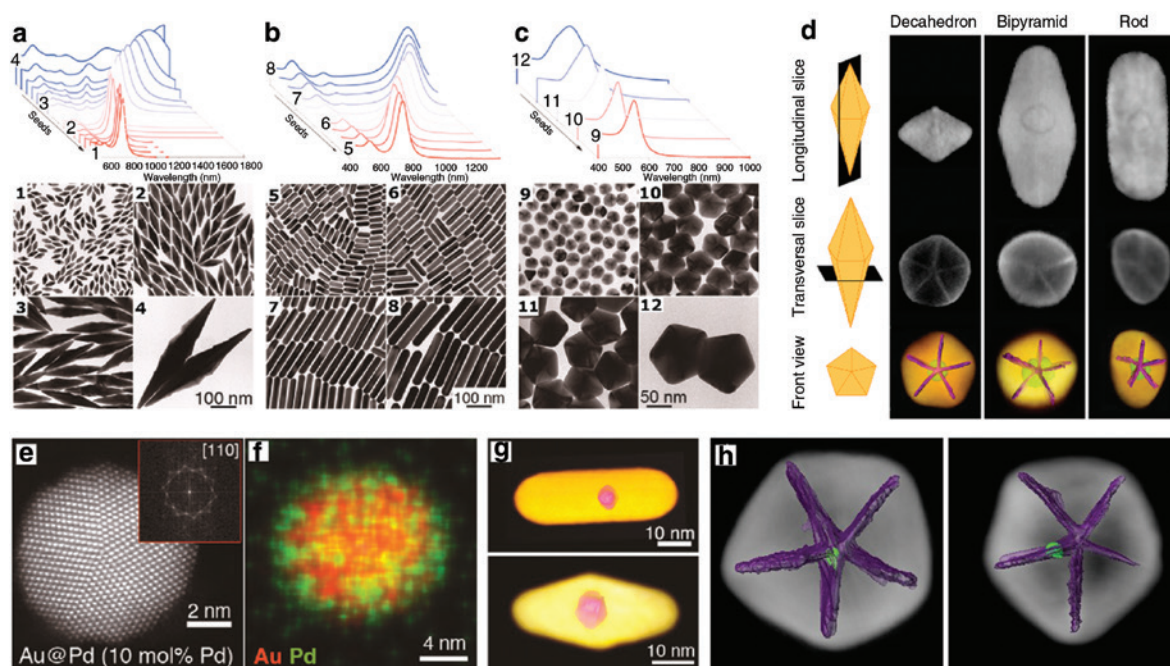


Fig. 4: High-yield synthesis of penta-twinned gold nanoparticles. (a–c) Effect of seed concentration on the growth of bipyramids (a), nanorods (b), and decahedra (c). Top: UV-vis-NIR spectra of colloids prepared with different seed concentrations. Bottom: representative TEM images of nanoparticles prepared in a single growth step from different amounts of seeds. The numeric labels indicate the correspondence of spectral and microscopy analysis. (d) Longitudinal orthoslices through the HAADF-STEM reconstruction (Top row), transversal orthoslices through the LAADF-STEM reconstruction, from which the twins can be segmented (Middle row), and the dose-efficient superimposition of the two analysis (Bottom row), of a decahedron (Left column), a bipyramid (Central column) and a nanorod (Right column) grown from Au/Pd seeds (Pd 20 mol%). (e) HAADF-STEM image of a thermally treated seed overgrown with palladium (10 mol%), preserving the crystal structure. (f) EDS mapping of Au@Pd (10 mol%) showing the outer distribution of Pd. (g) 3D visualization of the reconstructed volume of an individual nanorod (Top) and bipyramid (Bottom) obtained through the standard growth process using Au/Pd seeds, 10 and 50 mol% Pd for rods and bipyramids, respectively. (h) The position of the Pd seed inside Au bipyramids was determined using multimode tomography. The seed is located either at the connection point of the five twin planes (Left) or next to it (Right). Adapted with permission from Ref. [60, 64]. Copyright 2017 American Chemical Society.

for a single nanorod (Fig. 6a,d,e) [88]. Here, the experimental keystone is the ability to balance the energy delivered to the crystal lattice by the laser and the one dissipated through the surrounding medium in order to avoid drastic deformation of the nanorods (Fig. 6f–h) [89, 90]. This balance induced a slow reshaping of the particle towards a more thermodynamically favored product [91]. The final nanorod aspect ratio dispersity is as low as 2% (Fig. 6a), an outstanding improvement as compared to the starting material, which at best has shown a variation of 15%. Moreover, the process can be applied to nanorod colloids with longitudinal LSPR bands placed in any region of the spectra (Fig. 6b), and it was demonstrated as effective even when irradiating colloids with wide initial distribution in aspect ratio and size (Fig. 6c). The only limitations are the inevitable blue shift of the band associated with the refining process, and the availability of a laser with the correct wavelength. If extended to other shapes and materials, this approach holds the potential to pave the way towards a new era in the fabrication of plasmonic nanoparticles.

Plasmon hybridization and self-assembly

Self-assembly processes are ubiquitous in nature at all scales [92]. Apart from the creation of a certain degree of order, these phenomena are joined by three important characteristics: the balance of attractive

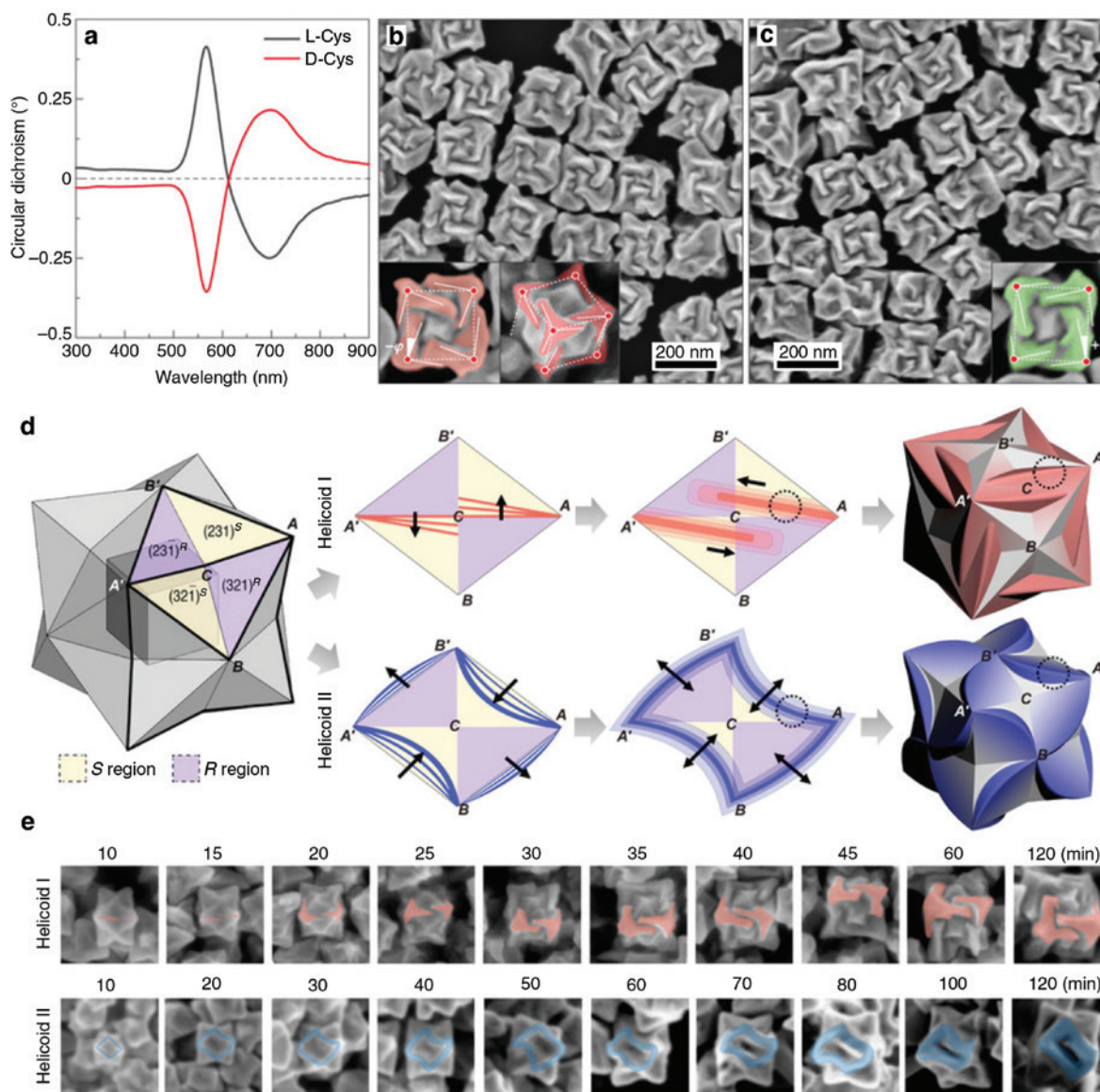


Fig. 5: (a) Opposite handedness of three-dimensional plasmonic helicoids controlled by cysteine chirality transfer and chiral morphology development mechanism. (a–c) Circular dichroism spectra (a) and SEM images of chiral nanoparticles synthesized using L- (black line, b) and D-Cysteine (red line, c). Insets: higher magnification images highlighting the edges (solid lines) tilted by an angle $\pm\phi$ with respect to the vertices (dots) and cubic outline (dashed lines). For L-Cysteine, both [100] (left) and [111] (right) directions are shown. (d) Schematic illustration of the time-dependent evolution of the chiral morphology. All models are viewed along the [110] direction. Starting from a {321}-indexed nanoparticle with an equal ratio of R and S regions, different R–S boundaries are split, thickened and distorted. (e) SEM images of helicoids I and II at different growth times. The chiral components that developed in into the final helicoid I and II are highlighted in red and blue, respectively. Adapted by permission from Ref. [73]. Copyright 2018 Springer Nature Publisher.

and repulsive interactions [93–96], the rational design of building blocks [97], and the generation of novel or enhanced properties [98, 99]. For plasmonics, the interest in self-assembly originates from the opportunity to control the interaction of the electron clouds of nanoparticles brought in close proximity within the range of few nanometers [100, 101]. In fact, plasmon coupling offers additional ways of tuning the optical response of plasmonic nanostructures [102]. Additionally, this leads to the formation of regions characterized by an extremely high electric field, called “hot-spots”, where the interacting nanoparticles are closest to each other [103]. As such, the last decade has seen intense activity in this field, with the development of various strate-

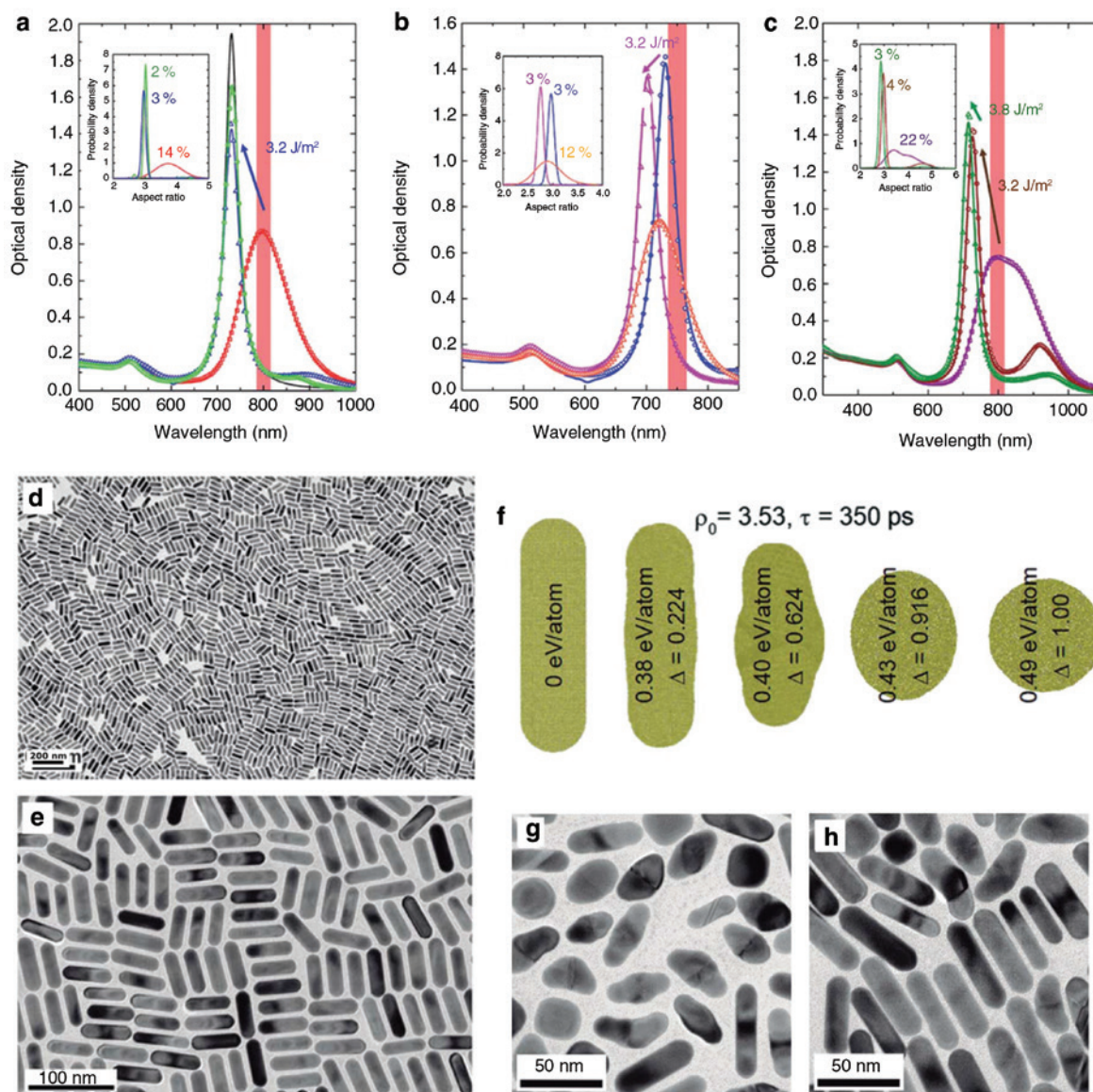


Fig. 6: Preparation of gold nanorod colloids with ultranarrow LSPRs by femtosecond laser-controlled reshaping. (a–c) Experimental (symbols) and fitted (lines) optical density spectra of colloids, before and after 1 h irradiation with (a) 800-nm 50-fs laser pulses 3.2 J/m² (red to blue); the spectrum of the purified irradiated colloid (green) nearly matches that calculated for a single particle (black). (b) 750-nm 50-fs laser pulses 3.2 J/m² (blue to purple). (c) 800-nm 50-fs laser pulses, 1 h at 3.2 J/m² (violet to brown) and 1 h at 3.8 J/m² (brown to green). Insets: aspect ratio probability densities derived from the optical fits. (d,e) Representative TEM images of reshaped nanorods at different magnifications, confirming narrow aspect ratio distribution and *quasi*-quantitative shape-yield. (f) Effect of total deposited energy on the evolution of gold nanorods aspect ratio. (g,h) Representative TEM image of reshaped nanorods upon irradiation with 5.1 J/m² [0.6 eV/atom, (e)], and 3.2 J/m² [0.38 eV/atom, (f)] for 1 h. Adapted from Ref. [88]. Reprinted with permission from AAAS.

gies for the production of complex structures using plasmonic building blocks, with promising applications in optical sensing of various analytes [104–106], single-molecule studies [107, 108], plasmonic-enhanced spectroscopies [109–111], metamaterials [112–114], and photovoltaics [115].

Recently, Liz-Marzán's group demonstrated the potential of these kinds of architectures for the sensing of biologically relevant analytes in complex matrixes. Gold nanorod supercrystals were fabricated using a template-mediated self-assembly (Fig. 7a–c), and their plasmonic properties were tuned to maximize the enhancement of the SERS signal [116, 117]. These nanoarchitectures were proposed to work in complex

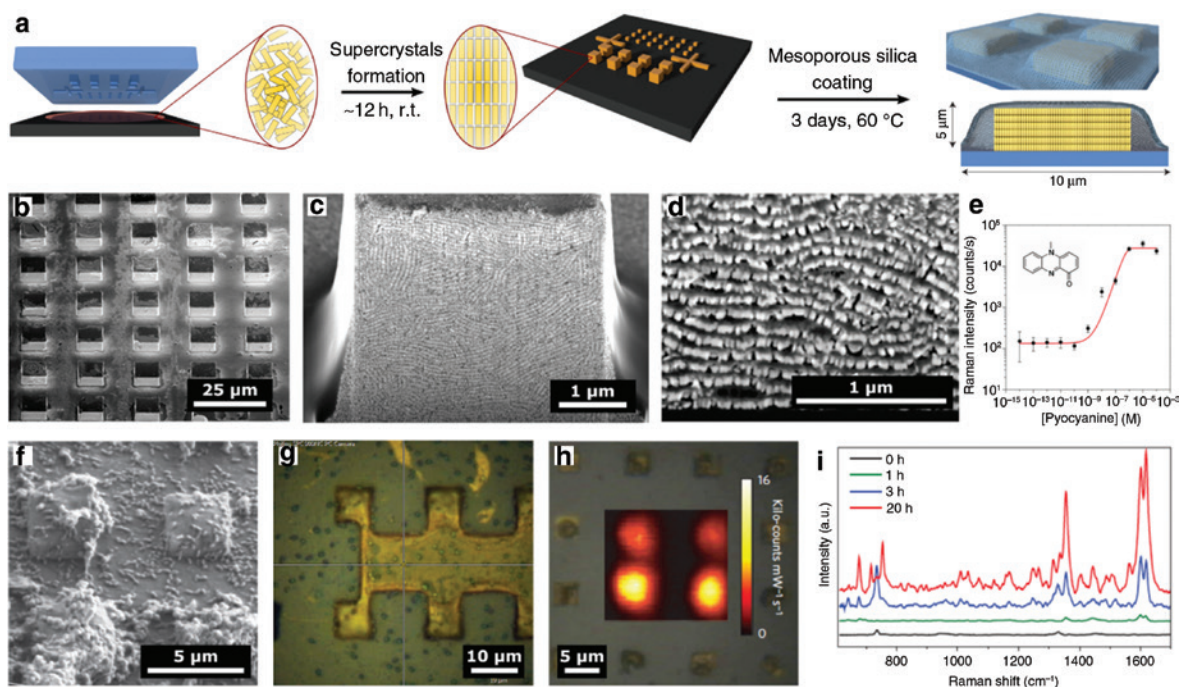


Fig. 7: Fabrication of plasmonic supercrystals and SERS in situ detection of quorum sensing signaling molecules. (a) Schematic representation of the gold nanorod-silica hybrid supercrystal fabrication process. (b–c) SEM image of a supercrystal obtained with a starting Au concentration of 375 mM (ca. 800-fold more concentrated than the initial nanorod dispersion) at different magnification. (d) SEM image of a gold nanorod-silica hybrid supercrystal cross-section. (e) Pyocyanin SERS detection using nanorod-silica hybrid supercrystals, showing a sub-nM limit of detection. (f,g) SEM (f) and optical image (g) of silica-coated Au nanorod supercrystals colonized by *Pseudomonas aeruginosa* after 20 h incubation. (h) SERS mapping of pyocyanin (1600 cm^{-1}) recorded at 20 h of growth. (i) Representative SERS spectra measured at 0, 1, 3 and 20 h (785 nm laser line, 0.98 kW cm^{-2} $50\times$ objective, and acquisition time $100\text{ }\mu\text{s}$). Adapted with permission from Refs. [111, 118, 119]. Copyright 2017 American Chemical Society (Ref. [111]). Published by The Royal Society of Chemistry (Ref. [118]). Copyright 2016 Springer Nature Publisher (Ref. [119]).

media such as living bacteria colonies, therefore a mesoporous silica layer was grown around the nanorod supercrystals in order to increase their structural stability, and to avoid proteins and other bulky contaminants reaching the sensing surface (Fig. 7d,e) [118]. Ultimately, these hybrid plasmonic superstructures were utilized for in situ, label-free SERS detection of pyocyanin (a quorum sensing signaling metabolite) in growing *Pseudomonas aeruginosa* biofilms (Fig. 7f–h) [119]. Additionally, this approach offers a significant improvement in temporal resolution, with pyocyanin detection within the first hour of biofilm growth (Fig. 7i) [120, 121].

From a thermodynamic perspective, it is important to distinguish two different kinds of processes: static and dynamic self-assembly. For static assembly, the particles will self-assemble into the most stable ordered structure upon thermodynamic equilibrium, whereas dynamic self-assembly (also called self-organization or dissipative self-assembly) occurs in non-equilibrium systems and disorder will occur once the external energy ceases to be dispensed (i.e. the assembly persists only if the system is dissipating energy) [122, 123]. These dynamic assemblies can lead to the creation of highly responsive systems capable of fast adaptation and integration into complex environments [124–126]. This can be extremely beneficial for plasmonic-enhanced spectroscopies. In fact, both irreproducibility and inhomogeneity of the signal over the sensing area are two major limitations that hinder the translation of hot-spot-based techniques into commercial products. In this frame, the introduction of dynamic self-assembly for controlling hot-spot formation can boost the development of robust sensing platforms. Velleman *et al.* assembled plasmonic nanoparticles into a self-healing, low-defect 2D film at a liquid-liquid interface, and were able to demonstrate the dynamic modulation of interparticle distance within the film using electrolytes or pH adjustments, manifesting sub-nanometer precision

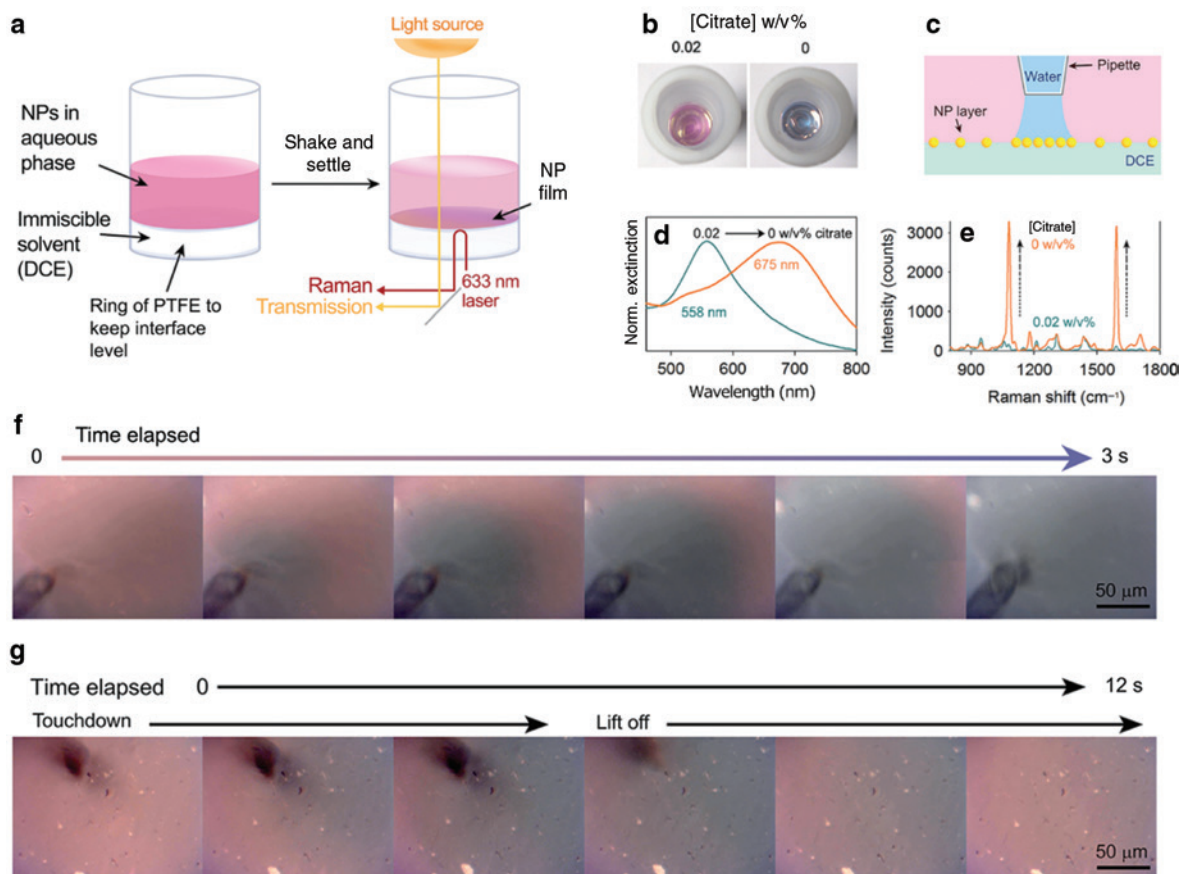


Fig. 8: Modulating plasmon coupling and SERS enhancement through dynamic self-assembly at the liquid-liquid interface. (a) Schematics of the nanoparticle film formation via emulsification of a nanoparticle aqueous solution with an immiscible solvent. The emulsion is allowed to settle, leaving a 2D array of nanoparticles at the liquid-liquid interface. (b) Photographs of the gold nanoparticle film taken from above, prepared at 0.02 w/v% citrate (left) and after reducing the citrate concentration to 0 w/v% (right). (c) Schematic of water delivery through a micropipette for localized modulation of nanoparticle spacing. (d) Extinction spectra of the gold nanoparticle film exhibiting a red-shift and broadening of the LSPR as the citrate is removed. (e) Raman spectra of the model analyte 4-mercaptobenzoic acid adsorbed onto the surface of the nanoparticles before (cyan) and after (orange) reduction in the citrate concentration. (f, g) Optical microscopy images extracted from a video as a micropipette was brought close to the nanoparticle film and water was injected just above the layer. (f) As the water is pumped in above the gold nanoparticle layer the film turns from a pink color to blue/gray. (g) Images displaying the self-healing properties of the film. The micropipette is lowered towards the interface of the film, which turns the film blue/gray. As the pipette is extracted away from the interface, the film is seen to return to its original pink color. Adapted with permission from Ref. [127] with permission of The Royal Society of Chemistry.

(Fig. 8a) [127, 128]. This ability to tailor the plasmonic properties on the same sample, allows for an unprecedented degree of control over hot-spot formation and SERS enhancement in real-time, and a more profound understanding of the assembly process (Fig. 8e). In particular, spherical nanoparticles are brought closer together upon reducing the citrate concentration, either by injecting water with a pipette, or replacing the entire aqueous phase with milli-Q water (Fig. 8b–d). Surprisingly, the proposed platform responds rapidly to environmental changes, and shows quick self-healing properties (Fig. 8f, g). Although this work has focused on model molecules only, its extension to more complex matrixes and analytes of interest can finally bridge the gap for the fabrication of a commercial SERS device.

The possibility of performing correlated studies at the level of a single nanoparticle is crucial toward the understanding and manipulation of optical phenomena at the nanometer scale [129, 130]. To this end, optical tweezing has proven to be a promising technique for analyzing single microscopic objects that are physically

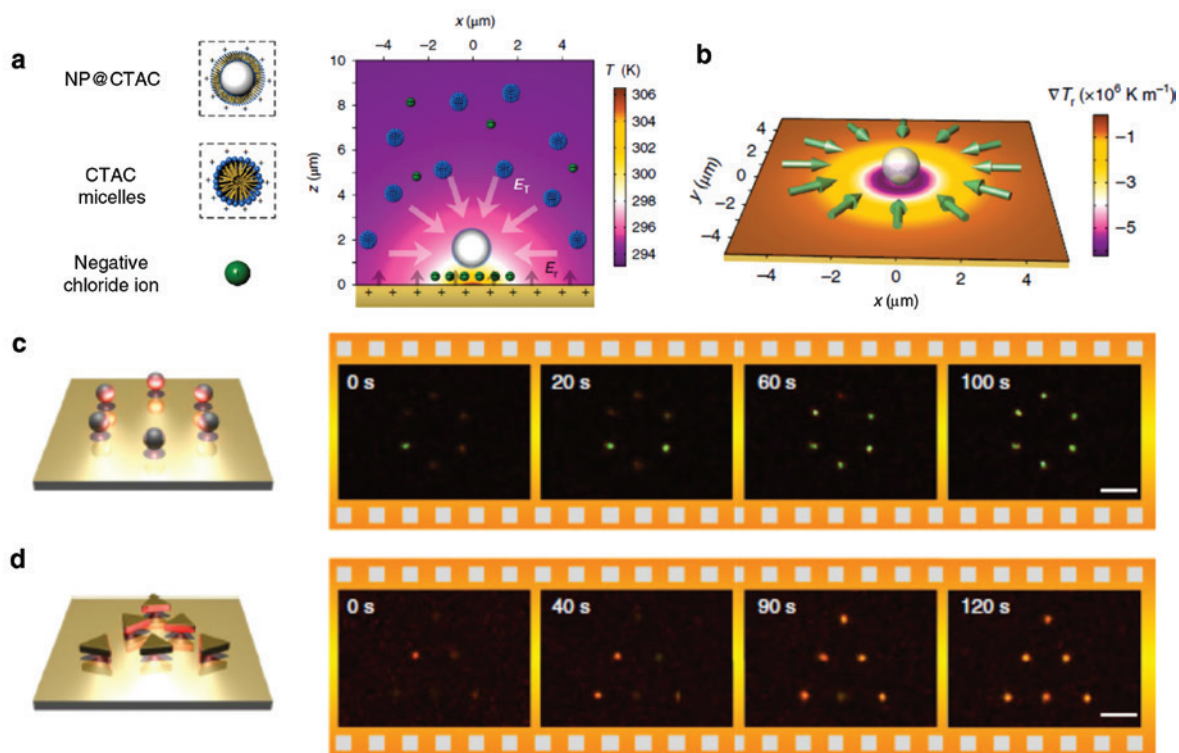


Fig. 9: Light-mediated optical trapping of single nanoparticles. (a) Steady ionic distribution under optical heating generates a thermoelectric field E_t for trapping the metal nanoparticle. The repulsive electric field E_r arises from the positive charges of the thermoplasmonic substrate and balances E_t . (b) Simulated in-plane temperature gradient ∇T_r and direction of the corresponding trapping force. The incident laser beam in (a,b) has a diameter of $2\ \mu\text{m}$ and an optical power of $0.216\ \text{mW}$. The green arrows in (b) show the direction of the trapping force. (c) Parallel trapping of six $100\ \text{nm}$ silver nanoparticles into a circular pattern. (d) Parallel trapping of six $140\ \text{nm}$ gold nanotriangles into a triangular pattern. Scale bars: $5\ \mu\text{m}$. Adapted with permission from Ref. [137]. Copyright 2018 Springer Nature Publisher.

held and moved exploiting their refractive index mismatch with the environment. This technique has been applied to a variety of systems, including quantum dots, single molecules, biological machinery, and whole cells [131, 132]. Although optical tweezing has also been demonstrated to successfully trap plasmonic nanoparticles with different sizes and shapes, there are still many limitations preventing its universal application [133, 134]. In particular, the heat generated upon excitation of the LSPR reduces the stability of the trap [135], limiting the technique to nanoparticles significantly smaller than the laser wavelength [136], and requires high laser power, potentially damaging the trapped object and the ligands on its surface [90]. In a series of recent publications, Zheng's group developed opto-thermoelectric nanotweezers (OTENT), overcoming the standard limitation of optical trapping for plasmonic objects, and demonstrating capture and manipulation of gold nanoparticles with single-particle resolution (Fig. 9) [137–139]. This method relies on the generation of a thermoelectric trapping field through optical heating, using a porous gold film and cationic surfactant, cetyltrimethylammonium chloride (Fig. 9a) [137]. In particular, the higher diffusion thermal coefficient of the positive micelles compared to the counter-ions induces the formation of a temperature gradient through laser irradiation, imposing a nonuniform micelle concentration [139]. This results in a temperature-dependent local electrostatic potential that generates an electric force on the charged gold nanoparticles, driving their migration toward the hot region (Fig. 9a,b). Moreover, the same principle can be exploited for mobilizing plasmonic nanoparticle assemblies over the surface, and can be easily parallelized to trap multiple particles simultaneously (Fig. 9c,d) [139]. The main advantages of this novel technique are the drastic reduction in laser power, the simple optics required, and the possibility of applying it to trap nanoparticles with different morphologies, sizes, and compositions.

Conclusions and outlook

This review illustrates how plasmonics remains an active and developing area of research, with a variety of phenomena that have yet to be explored or fully understood. From a synthetic perspective, the possibility of narrowing the nanoparticle size dispersity to the point of obtaining colloids of nearly identical objects could bridge a long-lasting gap that exists between nanochemistry and traditional synthetic chemistry, where molecules of a certain compound are undistinguishable. Furthermore, the harvesting of intrinsically chiral plasmons can open the door to new and exciting applications for metal nanoparticles, such as magneto-plasmonics (using the magnetic component of the plasmonic field) [140, 141], or new forms of enantioselective catalysis. Along with the addition of new particles, new strategies of self-assembly for greater control of hot-spot formation, distribution, and gap distance between interacting particles, could push the current limitations of plasmonics-based ultrasensitive sensing techniques including nano-electronics and quantum plasmonics [142]. Altogether, this review highlights a chemical perspective on the advancement of anisotropic particle synthesis, assembly, and applications. On a final note, the author would like to emphasize the importance of recognizing and embracing the interdisciplinary nature of this field. The combined efforts of chemists, physicists, biologists, and engineers will be crucial towards a deeper scientific understanding and the development of new applications.

Acknowledgements: I want to express my sincere gratitude to Prof. Luis M. Liz-Marzán, for his constant support during my PhD thesis, and for creating such a stimulating environment to do science, where I could work at the top of my possibilities. I thank Prof. Paul S. Weiss for accepting me in his group at UCLA as a postdoc, and for his mentorship and help in shaping my independent career. Finally, I would like to thank Jason N. Belling, Gail A. Vinnacombe, Liv K. Heidenreich and Drs. Guillermo González-Rubio and Naihao Chiang for their inputs and comments in the preparation of this manuscript. L. S. is currently the recipient of the American Italian Cancer Foundation Postdoctoral Fellowship. The content of this manuscript is solely the responsibility of the author.

References

- [1] Physics grand challenges – EPSRC website, <https://www.epsrc.ac.uk/research/ourportfolio/themes/physicalsciences/introduction/grandchallenges/> (accessed May 24, 2018).
- [2] P. Anderson. *Science* **177**, 393 (1972).
- [3] D. J. de Aberasturi, A. B. Serrano-Montes, L. M. Liz-Marzán. *Adv. Opt. Mater.* **3**, 602 (2015).
- [4] H. Chen, L. Shao, Q. Li, J. Wang. *Chem. Soc. Rev.* **42**, 2679 (2013).
- [5] J. Langer, S. M. Novikov, L. M. Liz-Marzán. *Nanotechnology* **26**, 322001 (2015).
- [6] X. Huang, S. Neretina, M. A. El-Sayed. *Adv. Mater.* **21**, 4880 (2009).
- [7] A. Guerrero-Martínez, S. Barbosa, I. Pastoriza-Santos, L. M. Liz-Marzán. *Curr. Opin. Colloid Interface Sci.* **16**, 118 (2011).
- [8] N. Li, P. Zhao, D. Astruc. *Angew. Chem. Int. Ed.* **53**, 1756 (2014).
- [9] S. E. Lohse, C. J. Murphy. *J. Am. Chem. Soc.* **134**, 15607 (2012).
- [10] K. Thorkelsson, P. Bai, T. Xu. *Nano Today* **10**, 48 (2015).
- [11] D. Thompson. *Gold Bull.* **40**, 267 (2007).
- [12] R. D. Tweney. *Perspect. Sci.* **14**, 97 (2006).
- [13] M. Faraday. *Philos. Trans. R. Soc. Lond.* **147**, 145 (1857).
- [14] M. Kociak, O. Stéphan. *Chem. Soc. Rev.* **43**, 3865 (2014).
- [15] C. Louis, O. Pluchery. *Gold Nanoparticles for Physics, Chemistry and Biology*, Imperial College Press, London (2012).
- [16] U. Kreibig, M. Vollmer. *Optical Properties of Metal Clusters*, Springer-Verlag, Berlin, Heidelberg (1995).
- [17] J. K. G. Dhont, G. Meier, D. Richter, R. Zorn, G. Vliegthart, G. Gompper. 46th IFF Spring School 2015 – Functional Soft Matter – Lecture Notes, Theorie der Weichen Materie und Biophysik, Neutronenstreuung, Weiche Materie (2015).
- [18] L. Novotny, B. Hecht. *Principles of Nano-Optics*, Cambridge University Press, Cambridge, UK (2012).
- [19] C. F. Bohren, D. R. Huffman. *Absorption and Scattering of Light by Small Particles*, John Wiley & Sons, Hoboken, NJ, USA (2008).
- [20] G. Mie. *Ann. Phys.* **330**, 377 (1908).

- [21] E. Le Ru, P. Etchegoin. *Principles of Surface-Enhanced Raman Spectroscopy: and Related Plasmonic Effects*, Elsevier, Amsterdam (2008).
- [22] D. Jeanmaire, R. Vanduyne. *J. Electroanal. Chem.* **84**, 1 (1977).
- [23] M. N. Sanz-Ortiz, K. Sentosun, S. Bals, L. M. Liz-Marzán. *ACS Nano* **9**, 10489 (2015).
- [24] S. Kawata. *Near-Field Optics and Surface Plasmon Polaritons*, pp. 163–187, Springer, Berlin, Heidelberg (2001).
- [25] E. Fort, S. Grésillon. *J. Phys. Appl. Phys.* **41**, 013001 (2008).
- [26] F. J. García de Abajo, A. Howie. *Phys. Rev. Lett.* **80**, 5180 (1998).
- [27] T. A. Gschneidner, Y. A. D. Fernandez, S. Syrenova, F. Westerlund, C. Langhammer, K. Moth-Poulsen. *Langmuir* **30**, 3041 (2014).
- [28] M. J. McClain, A. E. Schlather, E. Ringe, N. S. King, L. Liu, A. Manjavacas, M. W. Knight, I. Kumar, K. H. Whitmire, H. O. Everitt, P. Nordlander, N. J. Halas. *Nano Lett.* **15**, 2751 (2015).
- [29] M. Mayer, L. Scarabelli, K. March, T. Altantzis, M. Tebbe, M. Kociak, S. Bals, F. J. García de Abajo, A. Fery, L. M. Liz-Marzán. *Nano Lett.* **15**, 5427 (2015).
- [30] E. C. Dreaden, A. M. Alkilany, X. Huang, C. J. Murphy, M. A. El-Sayed. *Chem. Soc. Rev.* **41**, 2740 (2012).
- [31] M. Grzelczak, J. Pérez-Juste, P. Mulvaney, L. M. Liz-Marzán. *Chem. Soc. Rev.* **37**, 1783 (2008).
- [32] S. E. Lohse, C. J. Murphy. *Chem. Mater.* **25**, 1250 (2013).
- [33] T. K. Sau, C. J. Murphy. *J. Am. Chem. Soc.* **126**, 8648 (2004).
- [34] N. R. Jana, L. Gearheart, C. J. Murphy. *Adv. Mater.* **13**, 1389 (2001).
- [35] B. Nikoobakht, M. A. El-Sayed. *Chem. Mater.* **15**, 1957 (2003).
- [36] B. Lim, Y. Xia. *Angew. Chem. Int. Ed.* **50**, 76 (2011).
- [37] Y. Xia, Y. Xiong, B. Lim, S. E. Skrabalak. *Angew. Chem. Int. Ed.* **48**, 60 (2009).
- [38] L. M. Liz-Marzán. *Chem. Commun.* **49**, 16 (2013).
- [39] M. R. Langille, M. L. Personick, J. Zhang, C. A. Mirkin. *J. Am. Chem. Soc.* **134**, 14542 (2012).
- [40] M. H. Huang, C.-Y. Chiu. *J. Mater. Chem. A* **1**, 8081 (2013).
- [41] F. Kim, S. Connor, H. Song, T. Kuykendall, P. Yang. *Angew. Chem. Int. Ed.* **43**, 3673 (2004).
- [42] T. K. Sau, A. L. Rogach. *Adv. Mater.* **22**, 1781 (2010).
- [43] B. Wiley, Y. Sun, B. Mayers, Y. Xia. *Chem. – Eur. J.* **11**, 454 (2005).
- [44] Z. Quan, Y. Wang, J. Fang. *Acc. Chem. Res.* **46**, 191 (2013).
- [45] S. E. Lohse, N. D. Burrows, L. Scarabelli, L. M. Liz-Marzán, C. J. Murphy. *Chem. Mater.* **26**, 34 (2014).
- [46] L. Scarabelli, A. Sánchez-Iglesias, J. Pérez-Juste, L. M. Liz-Marzán. *J. Phys. Chem. Lett.* **6**, 4270 (2015).
- [47] S. Eustis, M. A. El-Sayed. *Chem. Soc. Rev.* **35**, 209 (2006).
- [48] L. C. Kennedy, L. R. Bickford, N. A. Lewinski, A. J. Coughlin, Y. Hu, E. S. Day, J. L. West, R. A. Drezek. *Small* **7**, 169 (2011).
- [49] A. R. Tao, S. Habas, P. Yang. *Small* **4**, 310 (2008).
- [50] R. Sardar, A. M. Funston, P. Mulvaney, R. W. Murray. *Langmuir* **25**, 13840 (2009).
- [51] H. Zhang, M. Jin, Y. Xiong, B. Lim, Y. Xia. *Acc. Chem. Res.* **46**, 1783 (2013).
- [52] M. Liu, P. Guyot-Sionnest. *J. Phys. Chem. B* **109**, 22192 (2005).
- [53] A. Gole, C. J. Murphy. *Chem. Mater.* **16**, 3633 (2004).
- [54] W. Niu, L. Zhang, G. Xu. *ACS Nano* **4**, 1987 (2010).
- [55] M. N. O'Brien, M. R. Jones, K. A. Brown, C. A. Mirkin. *J. Am. Chem. Soc.* **136**, 7603 (2014).
- [56] G. González-Rubio, T. M. de Oliveira, T. Altantzis, A. L. Porta, A. Guerrero-Martínez, S. Bals, L. Scarabelli, L. M. Liz-Marzán. *Chem. Commun.* **53**, 11360 (2017).
- [57] L. Scarabelli, M. Coronado-Puchau, J. J. Giner-Casares, J. Langer, L. M. Liz-Marzán. *ACS Nano* **8**, 5833 (2014).
- [58] L. Scarabelli, M. Grzelczak, L. M. Liz-Marzán. *Chem. Mater.* **25**, 4232 (2013).
- [59] L. M. Liz-Marzán, M. Grzelczak. *Science* **356**, 1120 (2017).
- [60] A. Sánchez-Iglesias, N. Winckelmans, T. Altantzis, S. Bals, M. Grzelczak, L. M. Liz-Marzán. *J. Am. Chem. Soc.* **139**, 107 (2017).
- [61] B. Goris, S. Bals, W. Van den Broek, E. Carbó-Argibay, S. Gómez-Graña, L. M. Liz-Marzán, G. Van Tendeloo. *Nat. Mater.* **11**, 930 (2012).
- [62] B. Goris, M. Meledina, S. Turner, Z. Zhong, K. J. Batenburg, S. Bals. *Ultramicroscopy* **171**, 55 (2016).
- [63] O. Ersen, I. Florea, C. Hirlimann, C. Pham-Huu. *Mater. Today* **18**, 395 (2015).
- [64] N. Winckelmans, T. Altantzis, M. Grzelczak, A. Sánchez-Iglesias, L. M. Liz-Marzán, S. Bals. *J. Phys. Chem. C* **122**, 13522 (2018).
- [65] S. Gómez-Graña, J. Pérez-Juste, R. A. Alvarez-Puebla, A. Guerrero-Martínez, L. M. Liz-Marzán. *Adv. Opt. Mater.* **1**, 477 (2013).
- [66] B. Nikoobakht, M. A. El-Sayed. *Langmuir* **17**, 6368 (2001).
- [67] D. K. Smith, B. A. Korgel. *Langmuir* **24**, 644 (2008).
- [68] X. Kou, S. Zhang, C.-K. Tsung, M. H. Yeung, Q. Shi, G. D. Stucky, L. Sun, J. Wang, C. Yan. *J. Phys. Chem. B* **110**, 16377 (2006).
- [69] N. Garg, C. Scholl, A. Mohanty, R. Jin. *Langmuir* **26**, 10271 (2010).
- [70] Y. Hu, L. Wang, A. Song, J. Hao. *Langmuir* **34**, 6138 (2018).
- [71] X. Ye, L. Jin, H. Caglayan, J. Chen, G. Xing, C. Zheng, V. Doan-Nguyen, Y. Kang, N. Engheta, C. R. Kagan, C. B. Murray. *ACS Nano* **6**, 2804 (2012).

- [72] X. Ye, C. Zheng, J. Chen, Y. Gao, C. B. Murray. *Nano Lett.* **13**, 765 (2013).
- [73] H.-E. Lee, H.-Y. Ahn, J. Mun, Y. Y. Lee, M. Kim, N. H. Cho, K. Chang, W. S. Kim, J. Rho, K. T. Nam. *Nature* **556**, 360 (2018).
- [74] W. Yan, L. Xu, C. Xu, W. Ma, H. Kuang, L. Wang, N. A. Kotov. *J. Am. Chem. Soc.* **134**, 15114 (2012).
- [75] A. Kuzyk, R. Schreiber, Z. Fan, G. Pardatscher, E.-M. Roller, A. Högele, F. C. Simmel, A. O. Govorov, T. Liedl. *Nature* **483**, 311 (2012).
- [76] Z. Fan, A. O. Govorov. *Nano Lett.* **10**, 2580 (2010).
- [77] M. J. Urban, P. K. Dutta, P. Wang, X. Duan, X. Shen, B. Ding, Y. Ke, N. Liu. *J. Am. Chem. Soc.* **138**, 5495 (2016).
- [78] A. Kuzyk, R. Schreiber, H. Zhang, A. O. Govorov, T. Liedl, N. Liu. *Nat. Mater.* **13**, 862 (2014).
- [79] C. F. McFadden, P. S. Cremer, A. J. Gellman. *Langmuir* **12**, 2483 (1996).
- [80] D. S. Sholl, A. Asthagiri, T. D. Power. *J. Phys. Chem. B* **105**, 4771 (2001).
- [81] F. Hubert, F. Testard, A. Thill, Q. Kong, O. Tache, O. Spalla. *Cryst. Growth Des.* **12**, 1548 (2012).
- [82] J. H. Song, F. Kim, D. Kim, P. Yang. *Chem. – Eur. J.* **11**, 910 (2005).
- [83] Q. Zhang, L. Han, H. Jing, D. A. Blom, Y. Lin, H. L. Xin, H. Wang. *ACS Nano* **10**, 2960 (2016).
- [84] E. Carbó-Argibay, B. Rodríguez-González, J. Pacifico, I. Pastoriza-Santos, J. Pérez-Juste, L. M. Liz-Marzán. *Angew. Chem. Int. Ed.* **46**, 8983 (2007).
- [85] M. J. Mulvihill, X. Y. Ling, J. Henzie, P. Yang. *J. Am. Chem. Soc.* **132**, 268 (2010).
- [86] S. Gómez-Graña, B. Goris, T. Altantzis, C. Fernández-López, E. Carbo-Argibay, A. G. Martínez, N. Almora-Barrios, N. Lopez, I. Pastoriza-Santos, J. Perez-Juste, S. Bals, G. Van Tendeloo, L. M. Liz-Marzán. *J. Phys. Chem. Lett.* **4**, 2209 (2013).
- [87] J. Becker, I. Zins, A. Jakab, Y. Khalavka, O. Schubert, C. Sönnichsen. *Nano Lett.* **8**, 1719 (2008).
- [88] G. González-Rubio, P. Díaz-Núñez, A. Rivera, A. Prada, G. Tardajos, J. González-Izquierdo, L. Bañares, P. Llombart, L. G. Macdowell, M. A. Palafox, L. M. Liz-Marzán, O. Peña-Rodríguez, A. Guerrero-Martínez. *Science* **358**, 640 (2017).
- [89] S. Link, C. Burda, B. Nikoobakht, M. A. El-Sayed. *J. Phys. Chem. B* **104**, 6152 (2000).
- [90] A. Babynina, M. Fedoruk, P. Kühler, A. Meledin, M. Döblinger, T. Lohmüller. *Nano Lett.* **16**, 6485 (2016).
- [91] C. J. Murphy, L. B. Thompson, A. M. Alkilany, P. N. Sisco, S. P. Boulos, S. T. Sivapalan, J. A. Yang, D. J. Chernak, J. Huang. *J. Phys. Chem. Lett.* **1**, 2867 (2010).
- [92] G. M. Whitesides, B. Grzybowski. *Science* **295**, 2418 (2002).
- [93] A. Sánchez-Iglesias, M. Grzelczak, T. Altantzis, B. Goris, J. Perez-Juste, S. Bals, G. Van Tendeloo, S. H. Donaldson Jr., B. F. Chmelka, J. N. Israelachvili, L. M. Liz-Marzán. *ACS Nano* **6**, 11059 (2012).
- [94] W. Ni, R. A. Mosquera, J. Pérez-Juste, L. M. Liz-Marzán. *J. Phys. Chem. Lett.* **1**, 1181 (2010).
- [95] S. Ni, J. Leemann, H. Wolf, L. Isa. *Faraday Discuss* **181**, 225 (2015).
- [96] C. Hamon, M. Postic, E. Mazari, T. Bizien, C. Dupuis, P. Even-Hernandez, A. Jimenez, L. Courbin, C. Gosse, F. Artzner, V. Marchi-Artzner. *ACS Nano* **6**, 4137 (2012).
- [97] M. Grzelczak, J. Vermant, E. M. Furst, L. M. Liz-Marzán. *ACS Nano* **4**, 3591 (2010).
- [98] G. M. Whitesides, M. Boncheva. *Proc. Natl. Acad. Sci.* **99**, 4769 (2002).
- [99] Y. A. D. Fernandez, T. A. Gschneidner, C. Wadell, L. H. Fornander, S. L. Avila, C. Langhammer, F. Westerlund, K. Moth-Poulsen. *Nanoscale* **6**, 14605 (2014).
- [100] L. D. Landau, J. S. Bell, M. J. Kearsley, L. P. Pitaevskii, E. M. Lifshitz, J. B. Sykes. *Electrodynamics of Continuous Media*, vol. 8, Elsevier, Oxford, England (1984).
- [101] E. Prodan. *Science* **302**, 419 (2003).
- [102] J. B. Lassiter, J. Aizpurua, L. I. Hernandez, D. W. Brandl, I. Romero, S. Lal, J. H. Hafner, P. Nordlander, N. J. Halas. *Nano Lett.* **8**, 1212 (2008).
- [103] Z. J. Wang, S. L. Pan, T. D. Krauss, H. Du, L. J. Rothberg. *Proc. Natl. Acad. Sci.* **100**, 8638 (2003).
- [104] A. D'Agostino, A. Taglietti, B. Bassi, A. Donà, P. Pallavicini. *J. Nanoparticle Res.* **16**, 1 (2014).
- [105] J. Wang, P. Zhang, C. M. Li, Y. F. Li, C. Z. Huang. *Biosens. Bioelectron.* **34**, 197 (2012).
- [106] L. Wang, Y. Zhu, L. Xu, W. Chen, H. Kuang, L. Liu, A. Agarwal, C. Xu, N. A. Kotov. *Angew. Chem. Int. Ed.* **49**, 5472 (2010).
- [107] N. Chiang, N. Jiang, D. V. Chulhai, E. A. Pozzi, M. C. Hersam, L. Jensen, T. Seideman, R. P. Van Duyne. *Nano Lett.* **15**, 4114 (2015).
- [108] N. Chiang, N. Jiang, L. R. Madison, E. A. Pozzi, M. R. Wasielewski, M. A. Ratner, M. C. Hersam, T. Seideman, G. C. Schatz, R. P. Van Duyne. *J. Am. Chem. Soc.* **139**, 18664 (2017).
- [109] A. Shiohara, Y. Wang, L. M. Liz-Marzán. *J. Photochem. Photobiol. C Photochem. Rev.* **21**, 2 (2014).
- [110] E. C. Le Ru, P. G. Etchegoin, M. Meyer. *J. Chem. Phys.* **125**, 204701 (2006).
- [111] L. Scarabelli, C. Hamon, L. M. Liz-Marzán. *Chem. Mater.* **29**, 15 (2017).
- [112] A. V. Kabashin, P. Evans, S. Pastkovsky, W. Hendren, G. A. Wurtz, R. Atkinson, R. Pollard, V. A. Podolskiy, A. V. Zayats. *Nat. Mater.* **8**, 867 (2009).
- [113] F. Garwe, U. Huebner, T. Clausnitzer, E.-B. Kley, U. Bauerschaefer. *Proc. SPIE*, **5955**, 59550T (2005).
- [114] K. L. Young, M. B. Ross, M. G. Blaber, M. Rycenga, M. R. Jones, C. Zhang, A. J. Senesi, B. Lee, G. C. Schatz, C. A. Mirkin. *Adv. Mater.* **26**, 653 (2014).
- [115] S. Mubeen, J. Lee, N. Singh, S. Krämer, G. D. Stucky, M. Moskovits. *Nat. Nanotechnol.* **8**, 247 (2013).
- [116] C. Hamon, S. Novikov, L. Scarabelli, L. Basabe-Desmonts, L. M. Liz-Marzán. *ACS Nano* **8**, 10694 (2014).

- [117] C. Hamon, S. M. Novikov, L. Scarabelli, D. M. Solís, T. Altantzis, S. Bals, J. M. Taboada, F. Obelleiro, L. M. Liz-Marzan. *ACS Photonics* **2**, 1482 (2015).
- [118] C. Hamon, M. N. Sanz-Ortiz, E. Modin, E. H. Hill, L. Scarabelli, A. Chuvilin, L. M. Liz-Marzán. *Nanoscale* **8**, 7914 (2016).
- [119] G. Bodelón, V. Montes-García, V. López-Puente, E. H. Hill, C. Hamon, M. N. Sanz-Ortiz, S. Rodal-Cedeira, C. Costas, S. Celiksoy, I. Pérez-Juste, L. Scarabelli, A. La Porta, J. Pérez-Juste, I. Pastoriza-Santos, L. M. Liz-Marzán. *Nat. Mater.* **15**, 1203 (2016).
- [120] L. Steindler, V. Venturi. *FEMS Microbiol. Lett.* **266**, 1 (2007).
- [121] J. K. Jansson. *Curr. Opin. Microbiol.* **6**, 310 (2003).
- [122] J. D. Halley, D. A. Winkler. *Complexity* **14**, 10 (2008).
- [123] M. Fialkowski, K. J. Bishop, R. Klajn, S. K. Smoukov, C. J. Campbell, B. A. Grzybowski. *J. Phys. Chem. B* **110**, 2482 (2006).
- [124] J. R. Green, A. B. Costa, B. A. Grzybowski, I. Szleifer. *Proc. Natl. Acad. Sci.* **110**, 16339 (2013).
- [125] K. V. Tretiakov, I. Szleifer, B. A. Grzybowski. *Angew. Chem.* **125**, 10494 (2013).
- [126] R. Zhang, D. A. Walker, B. A. Grzybowski, M. Olvera de la Cruz. *Angew. Chem.* **126**, 177 (2014).
- [127] L. Velleman, L. Scarabelli, D. Sikdar, A. A. Kornyshev, L. M. Liz-Marzán, J. B. Edel. *Faraday Discuss.* **205**, 67 (2017).
- [128] L. Velleman, D. Sikdar, V. A. Turek, A. R. Kucernak, S. J. Roser, A. A. Kornyshev, J. B. Edel. *Nanoscale* **8**, 19229 (2016).
- [129] K. W. Smith, J. Yang, T. Hernandez, D. F. Swearer, L. Scarabelli, H. Zhang, H. Zhao, N. A. Moringo, W.-S. Chang, L. M. Liz-Marzán, E. Ringe, P. Nordlander, S. Link. *J. Phys. Chem. C* **122**, 13259 (2018).
- [130] A. Joplin, S. A. Hosseini Jebeli, E. Sung, N. Diemler, P. J. Straney, M. Yorulmaz, W.-S. Chang, J. E. Millstone, S. Link. *ACS Nano* **11**, 12346 (2017).
- [131] J. R. Moffitt, Y. R. Chemla, S. B. Smith, C. Bustamante. *Annu. Rev. Biochem.* **77**, 205 (2008).
- [132] P. M. Bendix, L. Jauffred, K. Norregaard, L. B. Oddershede. *IEEE J. Sel. Top. Quantum Electron.* **20**, 15 (2014).
- [133] Z. Li, W. Mao, M. S. Devadas, G. V. Hartland. *Nano Lett.* **15**, 7731 (2015).
- [134] Z. Yan, M. Sajjan, N. F. Scherer. *Phys. Rev. Lett.* **114**, 143901 (2015).
- [135] P. V. Ruijgrok, N. R. Verhart, P. Zijlstra, A. L. Tchebotareva, M. Orrit. *Phys. Rev. Lett.* **107**, 037401 (2011).
- [136] C. Min, Z. Shen, J. Shen, Y. Zhang, H. Fang, G. Yuan, L. Du, S. Zhu, T. Lei, X. Yuan. *Nat. Commun.* **4**, 2891 (2013).
- [137] L. Lin, M. Wang, X. Peng, E. N. Lissek, Z. Mao, L. Scarabelli, E. Adkins, S. Coskun, H. E. Unalan, B. A. Korgel, L. M. Liz-Marzán, E.-L. Florin, Y. Zheng. *Nat. Photonics* **12**, 195 (2018).
- [138] L. Lin, J. Zhang, X. Peng, Z. Wu, A. C. Coughlan, Z. Mao, M. A. Bevan, Y. Zheng. *Sci. Adv.* **3**, e1700458 (2017).
- [139] L. Lin, X. Peng, M. Wang, L. Scarabelli, Z. Mao, L. M. Liz-Marzán, M. F. Becker, Y. Zheng. *ACS Nano* **10**, 9659 (2016).
- [140] I. S. Maksymov. *Rev. Phys.* **1**, 36 (2016).
- [141] J. Y. Chin, T. Steinle, T. Wehler, D. Dregely, T. Weiss, V. I. Belotelov, B. Stritzker, H. Giessen. *Nat. Commun.* **4**, 1599 (2013).
- [142] X. Chen, L. Jensen. *Nanoscale* **10**, 11410 (2018).